The enhancement of coseismic slip and ground motion due to the accretionary wedge and sedimentary layer in the 2011 Tohoku-Oki earthquake

Xian Li[1 2], Yihe Huang[3]

[1]Key Laboratory of Earth and Planetary Physics, Institute of Geology and Geophysics, Chinese Academy of Sciences, Beijing 100029, China.

[2]College of Earth and Planetary Sciences, University of Chinese Academy of Sciences, Beijing 100049, China.

[3]Department of Earth and Environmental Sciences, University of Michigan, Ann Arbor, MI 48109, USA.

Corresponding author: Xian Li (lixian@mail.iggcas.ac.cn)

Key Points:

- A co-existence of the accretionary wedge and sedimentary layer greatly enhances shallow coseismic slip in the 2011 Tohoku-Oki earthquake.
- For smaller earthquakes, the enhancement effects of the two structures on coseismic slip decrease as the up-dip rupture extent is deeper.
- A co-existence of the two structures amplifies and prolongs near-field ground motions.

Abstract

Low-velocity accretionary wedges and sedimentary layers overlaying continental plates are widely observed in the subduction zones where historical large earthquakes ($M_w \geq 8.5$) have occurred. It was observed that rupture of the 2011 M_w 9.0 Tohoku-Oki earthquake propagated to the trench with large coseismic slip on the shallow fault, but what caused the huge shallow slip remains a prominent problem. Here we explore how the two low-velocity structures, accretionary wedge and sedimentary layer, affect coseismic slip and near-fault ground motions during the 2011 Tohoku-Oki earthquake. Constrained by the observed seafloor deformation, we present a 2-D dynamic rupture model of the 2011 Tohoku-Oki earthquake with an accretionary wedge and a sedimentary layer. Compared to a homogeneous model with the same friction and stress parameters on the fault, we find that the co-existence of the accretionary wedge and sedimentary layer significantly enhances the shallow coseismic slip and amplifies ground accelerations near the accretionary wedge. We then investigate a plausible scenario of a smaller Tohoku-Oki earthquake when its rupture does not reach the accretionary wedge. The sedimentary layer slightly enhances the coseismic slip while the accretionary wedge has almost no influence for the smaller earthquake scenario, but both structures significantly amplify ground accelerations on the overriding plate. We suggest that a co-existence of an accretionary wedge and a sedimentary layer tends to enhance coseismic slip, but the enhancement effect decreases as the up-dip limit of rupture zones terminates at a larger depth.

Plain Language Summary

The accretionary wedge and sedimentary layer are two sediment structures widely existing in subduction zones. The low seismic velocities of the two structures can have a great impact on rupture processes and ground motions of subduction zone earthquakes. In the 2011 M_w 9.0 Tohoku-Oki earthquake, rupture propagated to the trench with large coseismic slip on the shallow fault. Our dynamic rupture simulations reveal that a co-existence of an accretionary wedge and a sedimentary layer in the northern Japan trench significantly enhances the shallow fault slip during the 2011 M_w 9.0 Tohoku-Oki earthquake. By simulating a suite of smaller earthquake scenarios, we find that the enhancement effects of an accretionary wedge and a sedimentary layer on fault slip decrease as the up-dip rupture extent is deeper. These structures also significantly amplify and prolong ground motions for both large and small earthquakes. Subduction zones that feature a co-existence of the two structures may have greater potential to accommodate large earthquakes due to their enhancement effects on fault slip.

1. Introduction

Sediments play a key role in the mechanical processes of subduction zones. In the collision margin where an oceanic plate subducts into a continental plate, material offscraped from the downgoing oceanic plate forms a wedge-shaped low-velocity sediment zone called an accretionary wedge. Accretionary wedges are widely observed in subduction zones (Table 1). For example, in the northern Japan trench where the 2011 Tohoku-Oki earthquake occurred, a wedge-shaped sedimentary unit with P-wave velocities of 2.0-4.0 km/s is located at the seaward end of the continental plate and extends to a depth greater than 13 km (Tsuru et al., 2002). The accretionary wedge in the eastern Nankai trough consists of five layers having seismic velocities of 1.8, 1.9-2.7, 2.8-3.5, 3.8-4.6, and 4.6-5.3 km/s (Nakanishi et al., 1998). In the Cascadia subduction zone, the accretionary wedge is wide from Vancouver to northern Oregon but is narrow from southern Oregon to northern California (Gulick et al., 1998). Along the Peru-Chile trench, the size of the frontal accretionary complex is variable, with accreted sediments appearing in the margin of south-central Chile but absenting in Peru (Flueh et al., 1998; Krabbenhöft et al., 2004).

Besides accretionary wedges, the sedimentary layers overlaying continental plates are common features in subduction zones, as shown by the map of *Total Sediment Thickness of the World's Oceans and Marginal Seas* (Divins, 2003). In Sumatra, Ryukyu, north Japan, Cascadia, and Costa Rica, nearshore deposits accumulated on the continental margins, making up the sedimentary layers with a thickness of several kilometers (Table 1). Taking the northern Japan trench, eastern Nankai trough, and middle Ryukyu trench as examples, the conceptual diagrams in Figure 1 demonstrate three simplified scenarios about the distribution of sediments on the overriding plate. In the northern Japan trench, both the accretionary wedge and sedimentary layer are observed. The eastern Nankai trough has an accretionary wedge but no sedimentary layer, whereas there are only sedimentary layers in the middle Ryukyu trench.

Table 1. Dimensions and P-wave velocities of accretionary wedges and sedimentary layers in subduction zones

Subduction Zone	Accretionary wedge		Sedimentary layer		Reference
	Width (km)	P-wave velocity (km/s)	Thickness (km)	P-wave velocity (km/s)	
Makran	>100	1.8-4.4	N/A	N/A	Kopp et al., 2000
Sumatra	30	3.0-3.9	3-5	2.0-3.0	Kopp et al., 2001
Ryukyu trench	N/A	N/A	9	1.8-4.7	Kodaira et al., 1996
Nankai trough	150	1.8-5.3	N/A	N/A	Nakanishi et al., 1998
North Japan	40-60	2.0-4.0	2	1.7-2.4	Tsuru et al., 2002; Kimura et al., 2012
South Kuril	10	2.4-3.7	1-2	1.9-2.1	Klaeschen et al., 1994
Central Kuril	N/A	N/A	1-2	1.9-2.2	Klaeschen et al., 1994
North Kuril	18	2.4-2.8	1-2	2.0-2.2	Klaeschen et al., 1994
Aleutians	20-30	2.5-4.5	2-3	2.0-3.0	Holbrook et al., 1999
Alaska	30	1.5-4.5	1-2	1.5-2.4	Brocher et al., 1994; von Huene et al., 1998
Cascadia	50-100	4.5-5.0	3-5	2.0-3.0	Gulick et al., 1998; Parsons et al., 1998
Costa Rica	N/A	N/A	2-4	2.2-4.0	Sallarès et al., 2001
Peru	N/A	N/A	1-3	1.7-3.0	Krabbenhöft et al., 2004
Central Chile	35-50	3.0-4.0	1-3	2.0-2.3	Flueh et al., 1998

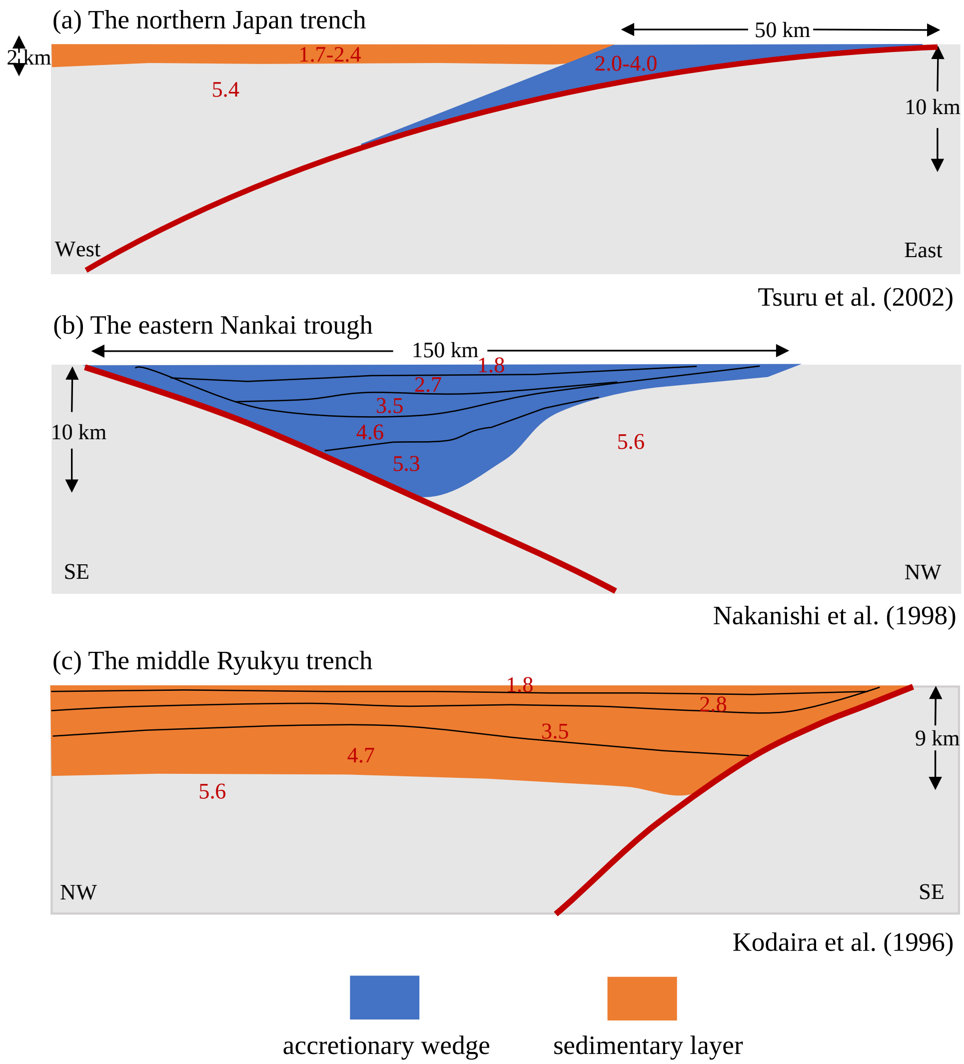

Figure 1. Conceptual diagrams showing sediment distribution on the overriding plate. (a) Co-existence of an accretionary wedge and a sedimentary layer. (b) Existence of an accretionary wedge only. (c) Existence of sedimentary layers only. Bold red curves represent the plate interface. The accretionary wedge is shown in blue, and the sedimentary layer is shown in orange. The numbers denote P-wave velocities (km/s) (Tsuru et al., 2002; Nakanishi et al., 1998; Kodaira et al., 1996).

In the last century, M_w 8.5 and above earthquakes occurred in the Sumatra, north Japan, Kuril, Kamchatka, Aleutians, Alaska, and south-central Chile subduction zones. These subduction zones all feature a co-existence of accretionary wedges and sedimentary layers, which can have a great impact on coseismic slip and ground motions of subduction zone earthquakes in two aspects: 1) The low-velocity material causes larger strain given the same stress according to Hooke's Law, which means larger coseismic slip at the base of accretionary wedges and larger deformation on the surface of sediments; 2) The reflected waves generated within these low-velocity structures can modulate rupture dynamics and induce high-frequency ground motions. Lotto et al. (2017) performed a series of numerical simulations and concluded that in most cases, larger and more compliant sedimentary prisms in subduction zones cause greater shallow slip. Ma and Hirakawa (2013) demonstrated that the Coulomb failure in the overriding wedge tends to give rise to significant seafloor uplift and depletion in the high-frequency radiation. Kubo et al. (2019) revealed that in the 2016 southeast off-Mie earthquake, the observed acceleration response spectra at periods of 0.5-8 s at seafloor stations largely exceeded values predicted by the empirical attenuation relationship due to the site amplification effect of shallow soft sediments. However, the combined effect of accretionary wedges and sedimentary layers on earthquake rupture processes and ground motions is yet unclear.

On 11 March 2011, the M_w 9.0 Tohoku-Oki earthquake occurred off the coast of northeast Japan, which brought heavy damage to human lives and structures. The earthquake occurred on a megathrust fault, where the Pacific plate subducts into the Okhotsk plate, in the northern Japan trench. Seafloor geodetic observations (Kido et al.,2011; Sato et al., 2011), ocean-bottom pressure gauge data (Ito et al., 2011), and multibeam bathymetric data (Fujiwara et al., 2011) indicated that the rupture of the Tohoku-Oki earthquake propagated to the trench. Slip inversions based on seismic recordings, geodetic data, tsunami data, and combinations of different data sets also supported huge coseismic slip in the shallow region of the plate boundary (Lay, 2018). However, most slip inversion models are based on an elastic homogeneous medium or a 1-D layer model without considering the low-velocity accretionary wedge and sedimentary layer. In the northern Japan trench, both the accretionary wedge and sedimentary layer are widely overlaying the continental plate (Tsuru et al., 2002). It is instrumental to understand how much these near-source structures contributed to the large seafloor deformation near the trench during the 2011 Tohoku-Oki earthquake. As the Seafloor Observation Network for Earthquakes and Tsunamis along the Japan Trench (S-net) has been monitoring offshore seismic activity, the accretionary wedges and sedimentary layers may contribute greatly to the observed seafloor ground motions from large subduction zone earthquakes as well.

A number of dynamic models have been proposed for the 2011 Tohoku-Oki earthquake to elucidate the rupture process, but they mainly focused on the effects of fault friction and stress state on slip distribution and rupture propagation. Kato and Yoshida (2011) proposed a mechanical model including strong asperity with higher effective normal stress and large characteristic slip distance on the shallow fault to explain the large shallow coseismic slip during the Tohoku-Oki earthquake. Duan (2012) conducted a suite of numerical experiments and found that a seamount in the up-dip direction of the hypocenter, characterized by higher static friction, lower pore fluid pressure, and higher initial stress, may cause large slip in the Tohoku-Oki earthquake. Mitsui et al. (2012) introduced a thermal pressurization mechanism to the models and suggested that the extremely large slip is caused by hydrothermal weakening on the fault plane. Huang et al. (2012, 2014) considered 2-D dynamic rupture models with linear slip-weakening friction, which reproduced three typical along-dip slip distributions during the Tohoku-Oki earthquake, and suggested that reflected waves inside the front wedge cause rupture to reach the trench. Noda and Lapusta (2013) proposed that the coseismic slip of the Tohoku-Oki earthquake can be explained by a model in which the fault patches are stable at low slip rates but experience shear-induced coseismic weakening. Kozdon and Dunham (2013) explored models with depth-dependent material properties and pointed out that waves reflected off the seafloor transmit large stress changes and might drive the rupture through the shallow velocity-strengthening region. Cubas et al. (2015) considered thermal pressurization in dynamic simulations by incorporating shear-induced temperature variations and pore fluid, which produced large shallow slip and the thousand-year recurrence time of Tohoku-Oki-like earthquakes.

Here, we aim at revealing the contributions of the accretionary wedge and sedimentary layer to the along-dip rupture propagation, coseismic slip, seafloor deformation, and ground motions by dynamic earthquake rupture simulations. As most seafloor deformation observation in the 2011 Tohoku-Oki earthquake concentrated in a direction perpendicular to the trench, we use a 2-D dynamic model to reproduce the observed deformation of the 2011 Tohoku-Oki earthquake by considering an accretionary wedge (aw) and a thin sedimentary layer (sed) overlaying the continental plate (aw-and-sed model) (Figure 1a). Compared to a homogeneous medium, our results suggest that the co-existence of the accretionary wedge and sedimentary layer greatly enhances the coseismic slip on the shallow fault and amplifies the peak ground accelerations at 0.1-0.5 Hz and 0.5-2.0 Hz near the accretionary wedge. The combined effect of the accretionary wedge and sedimentary layer is not a linear sum of the respective effects. We also simulate the rupture propagation and ground accelerations of a smaller Tohoku-Oki earthquake scenario whose rupture does not reach the accretionary wedge. In this scenario, we find that the sedimentary layer slightly enhances the coseismic slip while the accretionary wedge has almost no influence, but the co-existence of the two structures can greatly amplify ground accelerations on the overriding plate. We also discuss how our dynamic rupture models can be applied as reference scenarios to earthquake hazard analysis in global subduction zones where accretionary wedges or sedimentary layers exist.

2. Dynamic rupture models

2.1. The 2011 Tohoku-Oki earthquake model

We use a 2-D dynamic rupture model containing the main features of the northern Japan trench to reproduce the observed seafloor deformation of the 2011 Tohoku-Oki earthquake. In order to model the earthquake rupture process as realistically as possible, we apply observation data including seismic profile, geology survey, drilling site to constrain our model parameters (Tsuru et al., 2002; Kimura et al., 2012; Ujiie et al., 2013). A 200-km-wide fault with dip angles gradually changing from 6° at the surface to 16° at a depth of 50 km is embedded in an elastic half-space. An accretionary wedge is located within 50 km landward from the Japan trench axis on the surface and extends to 10 km in depth. A 2-km-thick sedimentary layer overlies the continental plate outside the accretionary wedge (Figure 1a). We use P-wave velocities of 2.0 km/s, 4.0 km/s, 5.4 km/s in the accretionary wedge, sedimentary layer, and surrounding zone respectively, in accordance with the seismic survey in the northern Japan trench (Tsuru et al., 2002). We set the Poisson's ratio to 0.25 and the density to 3000 kg/m^3 throughout the whole domain. The top of the model domain is a free surface, and an absorbing boundary is applied to the out-most margin to avoid artificial reflections. The hypocenter is located at a depth of 21 km (Chu et al., 2011) where we apply a time-weakening method (Andrews, 1985) to nucleate the earthquake. The dynamic rupture process is solved using SEM2DPACK, a software package simulating wave propagation and dynamic fracture using spectral element method (Ampuero, 2009).

We apply a linear slip-weakening friction law to the fault plane:

$$\begin{cases} \mu_s - \frac{\mu_s - \mu_d}{D_c} D & D < D_c \\ \mu_d & D \geq D_c \end{cases} \qquad (1)$$

Where μ_s is the static friction coefficient, μ_d is the dynamic friction coefficient, D_c is the critical slip distance, and D is slip. Since the velocity contrast between the accretionary wedge above the fault and rocks below the fault can lead to instability and ill-posedness due to normal stress perturbation during rupture propagation, we regularize the normal stress as follows (Huang et al., 2018):

$$\frac{d\sigma^*}{dt} = \frac{V^*}{D_\sigma} (\sigma - \sigma^*) \qquad (2)$$

Where σ^* is the effective normal stress, $V^* = 1$ is the reference slip rate, and $D_\sigma = 0.2$ is the reference distance.

In light of the frictional experiments on samples from the Japan Trench Fast Drilling Project (Fulton et al., 2013; Ujiie et al., 2013), we assume a low dynamic friction coefficient and shear stress near the trench. The static and dynamic friction coefficients in our models are 0.5 and 0.2, respectively. The normal stress linearly increases from 10 MPa at the surface to a constant value of 100 MPa below 5 km. The static (σ_s) and dynamic shear strengths (σ_d) are calculated by the product between the effective normal stress and the static and dynamic friction coefficients, respectively. The dynamic stress drop ($\Delta\sigma_d$) is the difference between the initial shear stress (τ_0) and dynamic shear strength. In our dynamic models, the $\Delta\sigma_d$ is nearly equal to the static stress drop which is the difference between the initial shear stress and the final stress. Positive and negative $\Delta\sigma_d$ represent regions that promote and prohibit rupture propagation, respectively, similar to the velocity-weakening and velocity-strengthening behaviors in rate-and-state friction models. We keep a uniform critical slip distance (D_c) of 2 m at depths above 4 km and 0.25 m around the nucleation zone to facilitate rupture nucleation. We also use small deep asperities with D_c of 0.25 m to reproduce high-frequency radiation of the 2011 Tohoku-Oki earthquake in the down-dip region (Figure 2a) (Huang et al., 2012).

We determine the initial shear stress τ_0 by fitting the simulated horizontal seafloor deformation of the aw-and-sed model with the observed data. Previous studies presented various types of slip distribution for the 2011 Tohoku-Oki earthquake (Lay, 2018), but most of them revealed large shallow slip. Here we use the slip distribution constrained by the observed seafloor deformation data that includes near-trench locations (Sato et al., 2011; Kido et al., 2011; Ito et al, 2011). It should be noted that the data may have large uncertainties in terms of the two points near the trench (~20 m). To reproduce the best-fitting deformation, τ_0 is 38 MPa in the nucleation zone and decreases to 18 MPa in the surrounding region. In the shallow portion of the fault, τ_0 increases to 44.6 MPa to fit the large horizontal deformation near the trench, and then linearly decreases to 1.2 MPa and remains constant till the surface (Figure 2a).

To isolate the contributions of the accretionary wedge and sedimentary layer on the coseismic slip and ground accelerations, we compare the aw-and-sed model to three models that only contain an accretionary wedge (aw-only model), a sedimentary layer (sed-only model), and homogeneous medium (homogeneous model) with the same friction and stress parameters as the aw-and-sed model.

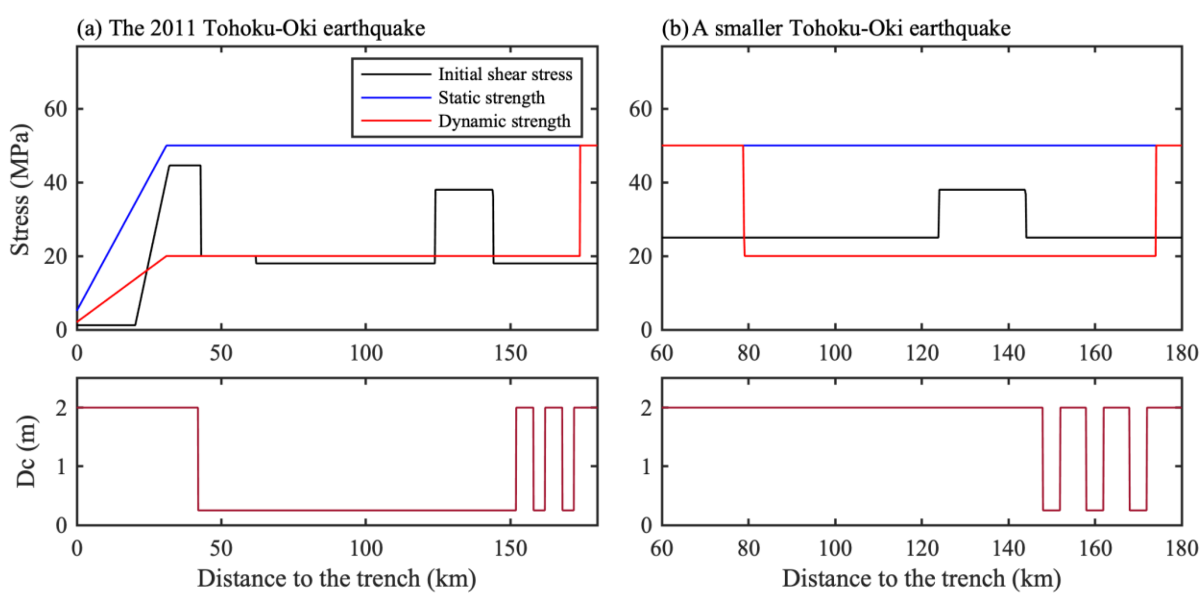

Figure 2. The surface projection of the along-dip distributions of initial shear stress, static strength, dynamic strength (top), and critical slip distance (bottom) for (a) the 2011 Tohoku-Oki earthquake and (b) a smaller Tohoku-Oki earthquake.

2.2. A smaller Tohoku-Oki earthquake model

For the smaller Tohoku-Oki earthquake whose rupture does not reach the accretionary wedge, we adopt the same model geometry as the 2011 Tohoku-Oki earthquake but change the friction and stress conditions on the fault. To constrain the rupture beneath the accretionary wedge, we increase the dynamic strength to the static strength level at depths above 11 km. In the rupture zone, the static and dynamic strengths are 50 and 20 MPa, respectively. We set the initial shear stress at 38 MPa in the nucleation zone and 25 MPa outside the nucleation zone. Similar to the 2011 Tohoku-Oki earthquake model, we use deep asperities in the down-dip region to represent the small-scale variation of frictional properties (Figure 2b).

3. Results

3.1. Slip and rupture dynamics of the 2011 Tohoku-Oki earthquake

The best-fitting aw-and-sed model of the 2011 Tohoku-Oki earthquake explains the large horizontal seafloor deformation at the two near-trench locations (Figure 3a). As the ratio between the horizontal and vertical deformation is mainly controlled by the fault-dip angle, the reproduced vertical deformation also has large values near the trench (Figure 3b). In the aw-and-sed model, the coseismic slip increases steeply from a trench-distance of 60 km to 35 km, with a peak slip reaching 83 m, similar to the maximum slip found by Iinuma et al. (2012) through the inversion of terrestrial GPS observations and seafloor geodetic data. Note that the aw-and-sed model results in slightly larger deformation than the observation at farther distances close to the hypocentral region, due to the dynamic stress drop required for successful nucleation given the frictional parameters used in our model. With the same friction and stress conditions, however, the homogeneous model produces a much flatter slip distribution despite large dynamic stress drop on the shallow fault. Slip in the homogeneous model is lower than that in the aw-and-sed model along the fault, especially in the shallow region, with the peak slip reduced by 25% (Figure 3c). As a result, the largest horizontal and vertical seafloor deformation are reduced by 29% and 22%, respectively (Figure 3a and 3b).

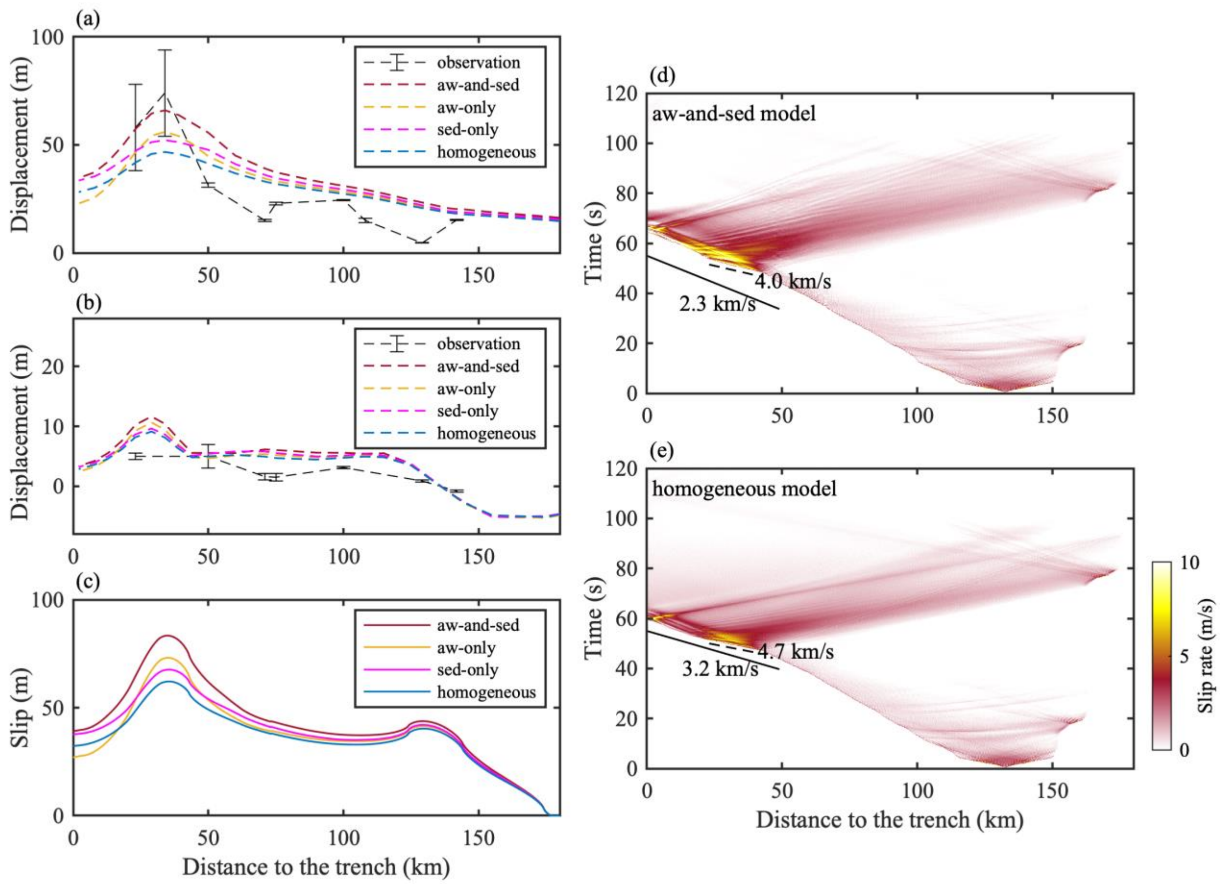

Figure 3. Surface deformation, fault slip, and slip rate during the 2011 Tohoku-Oki earthquake. (a) Horizontal surface deformation, (b) vertical surface deformation, and (c) surface projection of fault slip distributions produced by the aw-and-sed, aw-only, sed-only, homogeneous models. Spatiotemporal distributions of slip rate for (d) the aw-and-sed model and (e) the homogeneous model. Black solid lines represent shear wave speeds in the medium, 2.3 km/s in the accretionary wedge and 3.2 km/s in the homogeneous medium. The black dashed lines represent rupture velocities of 4.0 km/s and 4.7 km/s in the shallow portion of the aw-and-sed model and homogeneous model, respectively.

We also investigate the respective roles of the accretionary wedge and sedimentary layer on enhancing the fault slip and seafloor deformation. Both structures are found to greatly enhance the peak slip and deformation during the 2011 Tohoku-Oki earthquake, but the accretionary wedge has a dominant influence. The peak slip of the aw-only and sed-only models is 18% and 9% larger than that of the homogeneous model at a trench-distance of 35 km, respectively, while that of the aw-and-sed model is 34% larger at the same location (Figure 3c). The percentage of increased slip in the aw-and-sed model is also larger than the sum of the percentage of increased slip in the aw-only and sed-only models along the fault (Figure 4a). We conclude that the combined effect of the accretionary wedge and sedimentary layer on the coseismic slip is larger than a linear sum of the respective effects, and the same conclusion applies to the horizontal surface deformation (Figure 4b). We note that for the aw-only model, the fault slip decreases sharply in the shallow region and is smaller than that in the homogeneous medium within a trench-distance of 17 km (Figure 3c). Lotto et al. (2017) found that when prisms are large and have velocity-strengthening friction at the basement, increasing prism compliance reduces shallow slip. Our results suggest that the negative dynamic stress drop at the base of accretionary wedges also leads to a slip reduction compared to a homogeneous medium.

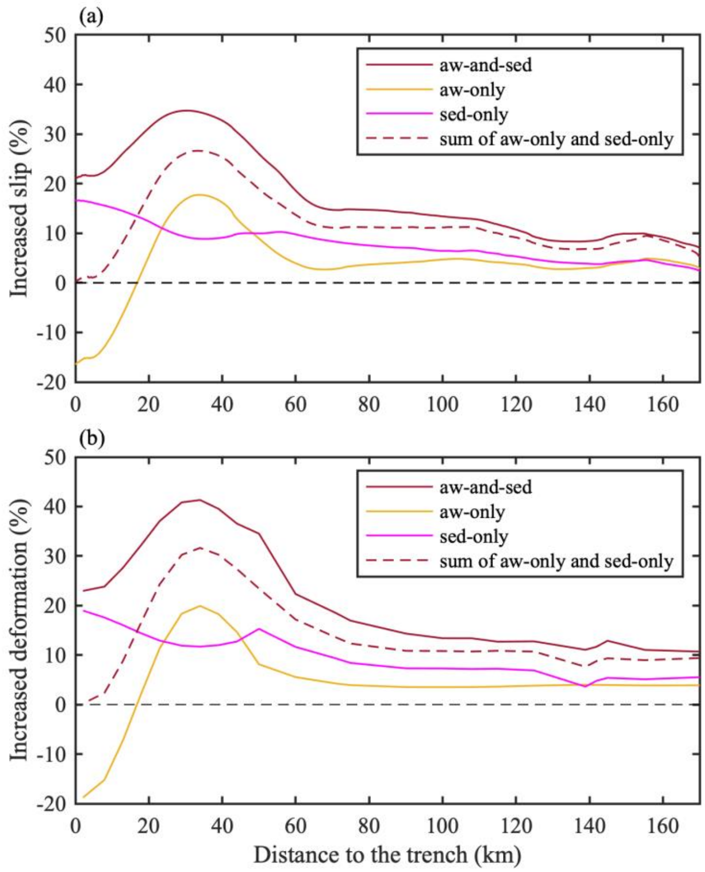

Figure 4. Percentage of increased fault slip and surface deformation in the non-homogeneous models compared with the homogeneous model in the 2011 Tohoku-Oki earthquake. (a) Percentage of increased slip. (b) Percentage of increased horizontal deformation. The red dashed lines are the total percentage of the aw-only and sed-only models.

Besides the effects on fault slip and surface deformation, the accretionary wedge also slows down shallow rupture propagation due to the lower S-wave speed in the accretionary wedge. Rupture propagates at an average speed of 2.5 km/s in the aw-and-sed model in the up-dip direction, compared to a speed of 3.4 km/s in the homogeneous medium. In both models, the shallow asperity with large dynamic stress drop causes local supershear rupture propagation (4 km/s in the aw-and-sed model and 4.7 km/s in the homogeneous model) in the up-dip direction (Figure 3d and 3e). Rupture then decelerates to subshear speeds as it propagates to the negative dynamic stress drop region.

3.2. Slip and rupture dynamics of a smaller Tohoku-Oki earthquake

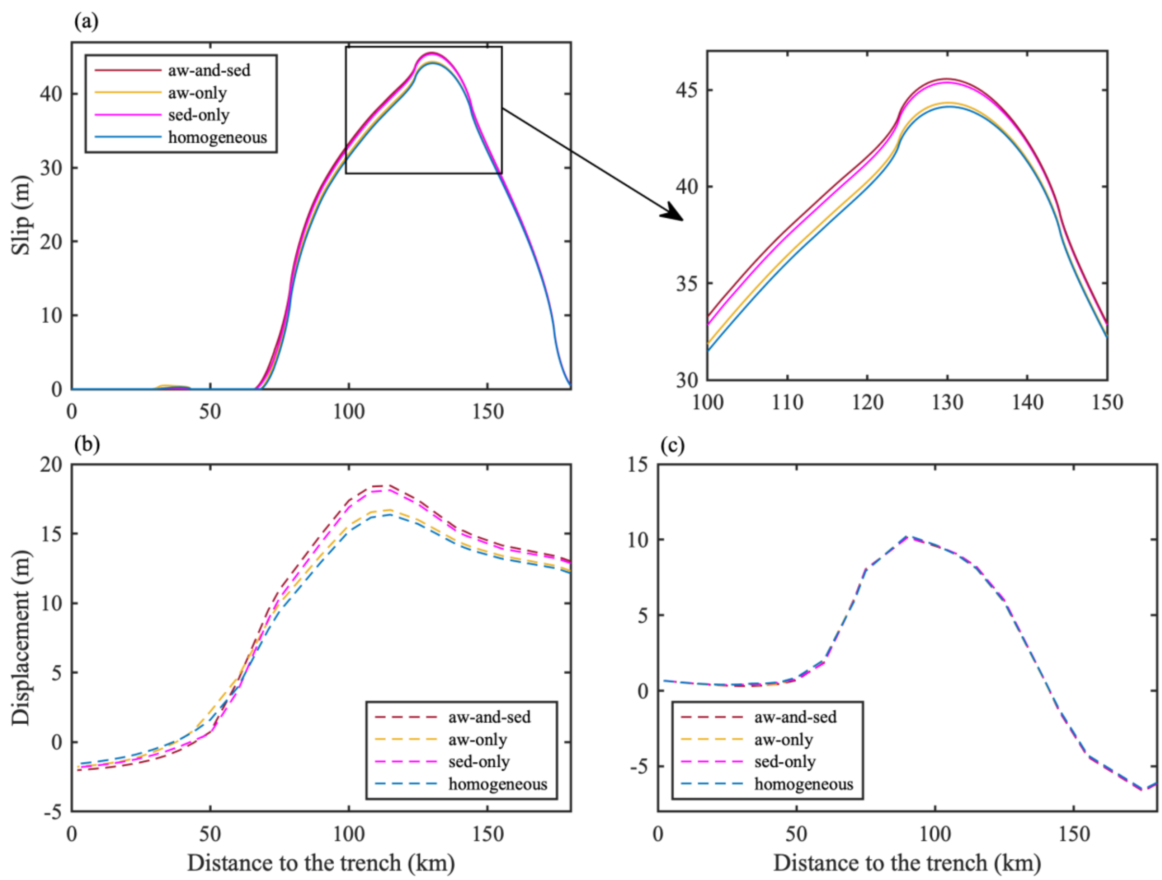

Figure 5. Fault slip and surface deformation produced by the aw-and-sed, aw-only, sed-only, homogeneous models during the smaller Tohoku-Oki earthquake. (a) Surface projection of fault slip distributions. An enlarged view of slip distributions between 100 and 150 km is displayed on the right side. (b) Horizontal surface deformation. (c) Vertical surface deformation.

In this section, we show that the effects of the accretionary wedge and sedimentary layer on coseismic slip and surface deformation strongly depend on the extent of shallow rupture, which translates into earthquake magnitude given the same hypocenter location. In the scenario of a smaller Tohoku-Oki earthquake that does not reach the accretionary wedge, a peak slip of ~45 m is located near the hypocenter for the aw-and-sed and homogeneous models (Figure 5a). The peak slip in the aw-and-sed model is 3% larger than that in a homogeneous medium (Figure 5a), which is significantly smaller than the 34% for the 2011 Tohoku-Oki earthquake that reached the accretionary wedge. The peak horizontal deformation has a 13% increase, but there is almost no difference in the vertical deformation (Figure 5b and 5c).

Comparing the slip distributions of the aw-and-sed, aw-only, sed-only, and homogeneous models, we note that the difference between the aw-only and homogeneous models is nearly undistinguishable for the smaller Tohoku-Oki earthquake, but the slip of the aw-and-sed and sed-only models is slightly larger than that of the homogeneous model near the hypocenter (Figure 5a). Hence, the aw-and-sed and sed-only models have larger horizontal deformation than the homogeneous model near the epicenter (Figure 5b). These results imply that for a smaller earthquake that does not reach the accretionary wedge, the accretionary wedge has almost no impact on the coseismic slip and surface deformation, and the increased slip and deformation in the aw-and-sed model mainly comes from the sedimentary layer.

3.3. Effects of the accretionary wedge and sedimentary layer on ground accelerations

We find that the co-existence of the accretionary wedge and sedimentary layer prolongs ground acceleration durations and amplifies peak ground accelerations, but the combined effect behaves differently depending on the shallow rupture extents of earthquakes. In the case of the 2011 Tohoku-Oki earthquake, the ground acceleration durations in the aw-and-sed model are significantly prolonged as shown in the accelerograms recorded at two stations inside and outside the accretionary wedge (Figure 6a). To quantify the ground acceleration amplification, the amplification factor is defined as a ratio of peak ground accelerations between non-homogeneous and homogeneous models. We calculate the average amplification factors in two frequency ranges: 0.1-0.5 Hz, 0.5-2.0 Hz. We find that for all stations on the overriding plate, the ground accelerations of the aw-and-sed model are significantly amplified at both 0.1-0.5 Hz and 0.5-2.0 Hz (Figure 6b). The maximum amplification effects for both frequency ranges happen in the vicinity of the accretionary wedge where the combined effect of the accretionary wedge and the sedimentary layer is greater than their linear sum. Inside the accretionary wedge, the amplification effect on the ground acceleration at 0.5-2.0 Hz is larger than at 0.1-0.5 Hz (Figure 6b).

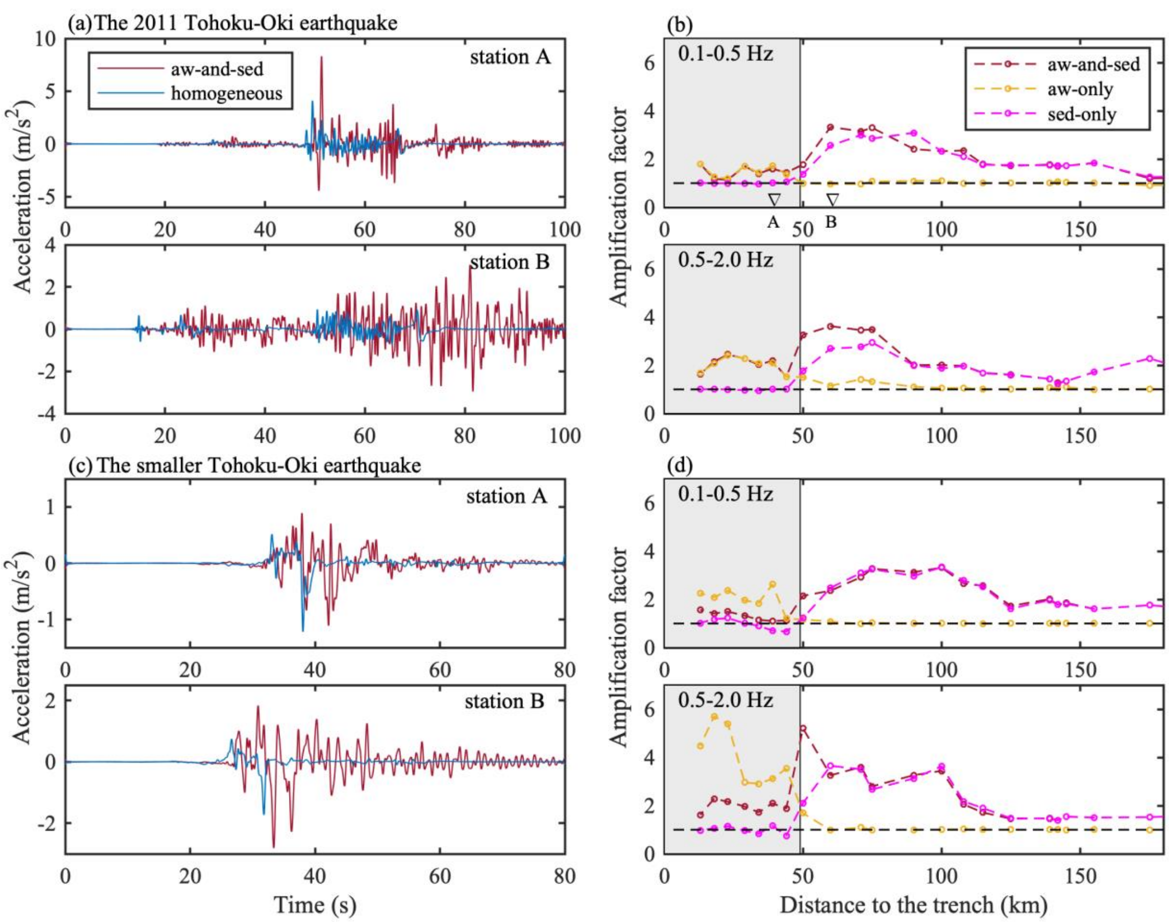

Figure 6. (a) Comparisons of accelerograms between the aw-and-sed and homogeneous models; (b) Averaged amplification factors for two frequency ranges at 0.1-0.5 Hz and 0.5-2.0 Hz produced by the three non-homogeneous models during the 2011 Tohoku-Oki earthquake. The shaded zone is the region inside the accretionary wedge. Black dashed lines represent a value of 1. A and B are stations located inside and outside the accretionary wedge, respectively. (c) and (d) have the same representation as (b) and (d), respectively, but for the smaller Tohoku-Oki earthquake.

For the smaller earthquake, although the accretionary wedge and sedimentary layer have a minimal influence on the fault slip, they can greatly enhance ground accelerations. However, the combined effect on the ground acceleration amplification is not always larger than the respective effects. Similar to the 2011 Tohoku-Oki earthquake, the aw-and-sed model produces longer durations at stations inside and outside the accretionary wedge (Figure 6c). In the aw-and-sed model, the maximum amplification effect on the ground acceleration at 0.1-0.5 Hz is located outside the accretionary wedge where the sedimentary layer has a major contribution (Figure 6d top). The maximum amplification factor at 0.5-2.0 Hz happens at the landward edge of the accretionary wedge where the combined effect of the accretionary wedge and the sedimentary layer is significantly greater than their linear sum (Figure 6d bottom).

We notice that for all the stations inside the accretionary wedge, the amplification factors of the aw-and-sed model are obviously smaller than those of the aw-only model, with the ground accelerations at 0.5-2.0 Hz being greatly suppressed in particular (Figure 6d bottom). Thus, for a smaller earthquake, the existence of a sedimentary layer may weaken the amplification effect of the accretionary wedge on ground accelerations inside the accretionary wedge, which may be attributed to wave interference between the two structures.

4. Discussion

4.1. Implications for stress drop estimation of the 2011 Tohoku-Oki earthquake

Stress release and accumulation on faults are essential to assess regional earthquake hazards. As an important parameter in controlling the source mechanism, stress drop during the 2011 Tohoku-Oki earthquake has been investigated by different methods. These studies consider a homogeneous medium, a 1-D layered medium without sedimentary layers, or a 1-D layered medium with sedimentary layers. Brown et al. (2015) estimated a mean stress drop of 2.3 ± 1.3 MPa and a peak value of as high as 40 MPa from 40 rupture models of the 2011 Tohoku-Oki earthquake assuming a uniform rigidity of 40 GPa. Assuming a 1-D model without sediment structures, Xie and Cai (2018) constrained an average stress drop of 6.3 MPa from stress inversion of the observed coseismic deformation. Koketsu et al. (2011) calculated an average stress drop of 4.8 MPa from the source model constructed through joint inversion of teleseismic, strong motion, and geodetic datasets with sedimentary layers considered in velocity structure.

Here our best-fitting aw-and-sed model reveals an average stress drop of 2.5 MPa and a maximum stress drop of 25 MPa on the shallow asperity in the 2011 Tohoku-Oki earthquake (Figure S1). However, to reproduce the same observed peak deformation near the trench, the maximum stress drop on the shallow asperity is ~27 MPa, 27MPa, and 30 MPa for the aw-only, sed-only, and homogeneous models, respectively (Figure S1). The stress drop on the shallow fault evaluated from the fault slip or directly from the surface deformation can be overestimated when accretionary wedge and sedimentary layer are not considered, as the co-existence of the two structures greatly enhances the coseismic slip during the 2011 Tohoku-Oki earthquake. Our results also suggest that for other large megathrust earthquakes that reach the accretionary wedge, stress drop estimated for a homogeneous medium may also be overestimated, especially in the peak slip region.

4.2. Frequency-dependent effects on strong ground motions due to accretionary wedges

Low-velocity accretionary wedges have a great impact on ground motion durations and amplitudes, which can strongly depend on ground motion frequencies. For example, accretionary wedges can lead to longer durations of long-period (>10 s) ground motions, due to the surface waves generated from the seaward edge of accretionary wedges or the reverberations of seismic waves within accretionary wedges (Guo et al., 2016; Kaneko et al., 2019). Kubo et al. (2019) observed that in the 2016 southeast off-Mie earthquake, the offshore acceleration response spectra at periods of 0.5-8 s largely exceeds values obtained from the empirical attenuation relationship while that at shorter periods of 0.12 and 0.25 s follows the empirical relationship. The results were interpreted as a large site amplification effect due to an accretionary wedge.

Our results show that in both the 2011 Tohoku-Oki earthquake and smaller earthquake, the accretionary wedge elongates the near-field ground acceleration durations and amplifies the ground accelerations at both 0.1-0.5 Hz and 0.5-2.0 Hz. The amplification effect inside the accretionary wedge exhibits distinct frequency-dependence, particularly for the smaller earthquake. Ground accelerations at 0.5-2.0 Hz are more amplified than ground accelerations at 0.1-0.5 Hz in our aw-only models (Figure 6d), which suggests that dynamic wave interaction inside an accretionary wedge can cause more ground acceleration amplification at high frequencies.

4.3. Implications for global megathrust earthquakes

In the last century, besides the northern Japan trench, M_w 8.5 and above earthquakes also occurred in the Aleutians, Alaska, Kuril, Kamchatka, south-central Chile, and Sumatra subduction zones. These subduction zones all feature a co-existence of accretionary wedges and sedimentary layers. The two structures could be major factors in controlling large subduction zone earthquakes. Wells et al. (2003) illustrated that rupture zones of great subduction zone earthquakes tend to underlie the forearc basins. Most seaward part of an accretionary wedge exhibits a velocity-strengthening behavior, which is generally thought to impede up-dip rupture (Wang & Hu, 2006). Ma and Nie (2019) showed that coseismic yielding of plentiful sediments in the northern Japan trench margin can induce large inelastic uplift and diminish slip near the trench. However, Gulick et al. (2011) suggested that the accreted sediments near the Sunda trench were dewatered and compacted, which allowed a velocity-weakening behavior and hence facilitated the rupture of the 2004 M_w 9.2 Sumatra-Andaman earthquake to the trench. Lotto et al. (2017) pointed out that more compliant accretionary prisms in most cases cause greater shallow fault slip, but larger prisms with velocity-strengthening friction reduce slip.

Our results suggest that accretionary wedges and sedimentary layers tend to enhance coseismic fault slip, but the enhancement effects decrease as the shallow negative dynamic stress drop ($\Delta\sigma_d$) region reaches a larger depth. The negative $\Delta\sigma_d$ region acts as a barrier prohibiting rupture propagation and thus affects rupture extents. The schematic diagrams in Figure 7 summarize the respective roles of an accretionary wedge and a sedimentary layer on fault slip. When the $\Delta\sigma_d$ is positive on the entire fault, a sedimentary layer or an accretionary wedge can greatly enhance fault slip (Figure 7a and 7b). If the $\Delta\sigma_d$ is negative beneath the outer wedge, which causes slip to decrease near the trench, a sedimentary layer or an accretionary wedge greatly enhances the peak slip, but the accretionary wedge leads to a sharper decrease in the slip near the trench (Figure 7c and 7d). As the shallow negative $\Delta\sigma_d$ region extends to a larger depth, causing rupture to terminate before arriving the trench, the enhancement effects of a sedimentary layer and an accretionary wedge on peak slip diminish (Figure 7e and 7f). As the extent of the negative $\Delta\sigma_d$ region is even deeper, a sedimentary layer slightly enhances fault slip, and an accretionary wedge has almost no influence (Figure 7g and 7h).

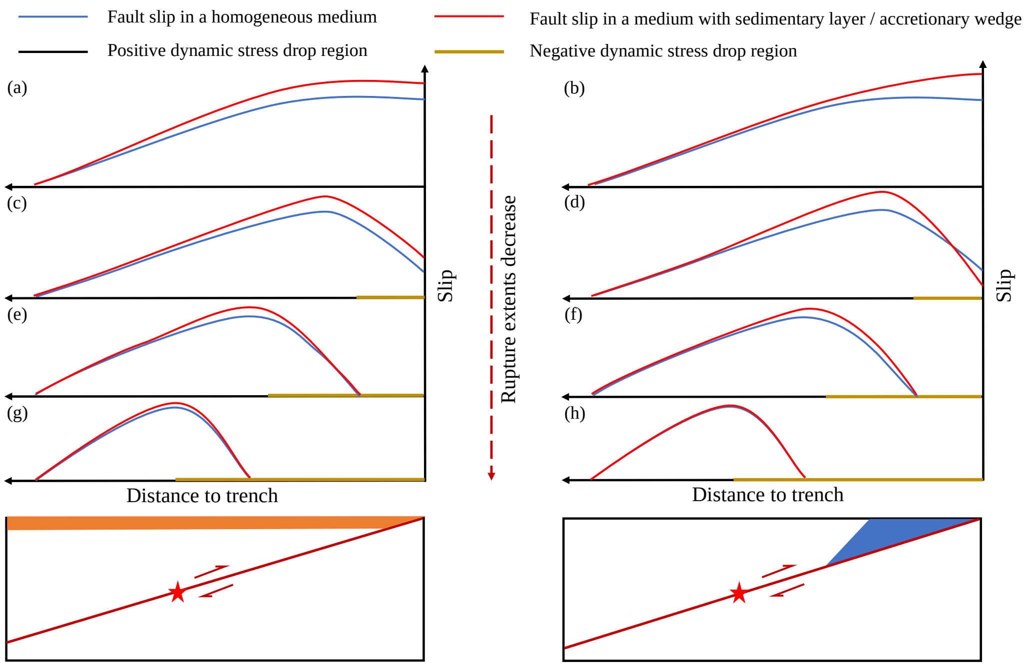

Figure 7. Schematic diagrams showing the respective effects of a sedimentary layer and an accretionary wedge on coseismic slip. The left column: comparisons of slip distribution between a homogeneous medium and a medium with a sedimentary layer. The right column: comparisons of slip distribution between a homogeneous medium and a medium with an accretionary wedge. Rupture extents decrease from top to bottom, which is controlled by the extent of the negative dynamic stress drop region.

The existence of accretionary wedges and sedimentary layers may allow subduction zones to have a greater potential to accommodate large earthquakes due to their enhancement effects on fault slip. In the 2004 M_w 9.2 Sumatra-Andaman earthquake, the coseismic rupture occurred largely beneath the accretionary prism in the southern part of the rupture area (Gulick et al., 2011). The upper bound of the coseismic slip during the 2010 M_w 8.8 Chile earthquake reached the toe of the accretionary prism with peak slips near the trench (Yue et al., 2014). The up-dip limit of the 1960 M_w 9.5 great Chile earthquake extends further seaward (Contreras-Reyes et al., 2010). The accretionary wedges and sedimentary layers may have played important roles in enhancing the shallow slip during these large earthquakes. In Cascadia where great earthquakes are the most likely to occur in the Pacific Northwest United States, wide accretionary wedges and sedimentary layers cover the continental plate (Gulick et al., 1998; Parsons et al., 1998). Our results suggest that future studies of Cascadia megathrust earthquakes should consider the effects of the two structures as well.

Since our focus is to evaluate the influence of accretionary wedges and sedimentary layers on the along-dip rupture process, 2-D models that do not account for along-strike variations are used in this work. In the rupture zone of the 2011 Tohoku-Oki earthquake, the wedge-shaped sediments appear in the northern area of the epicenter with dimensions varying along the Japan trench, but in the southern area, the sediments extend in the down-dip direction as a channel-like unit (Tsuru et al., 2002). Future numerical models should be directed towards 3-D rupture simulations to address the influence of along-strike heterogeneity on rupture features. On the other hand, we analyze the effects of the accretionary wedge and sedimentary layer on coseismic slip and ground motions assuming purely elastic properties. However, the nature of an accretionary wedge or a sedimentary layer can have viscoelastic and plastic behaviors, which may diminish slip and reduce surface deformation (Ma & Nie, 2019). Since the effect of sedimentary structures should be a combination of elastic and inelastic effects, whether it promotes fault slip depends on which behavior is in a dominant role. A more realistic approximation of accretionary wedges and sedimentary layers in future works is the incorporation of viscoelasticity and plasticity.

5. Conclusions

Our dynamic rupture simulations for the 2011 Tohoku-Oki earthquake show that the co-existence of the accretionary wedge and sedimentary layer significantly enhances the coseismic slip in the shallow region and greatly amplifies the ground accelerations near the accretionary wedge. In subduction zones having both an accretionary wedge and a sedimentary layer, the combined effect of the two structures on fault slip is larger than the linear sum of respective effects. However, the enhancement effect on fault slip decreases as the up-dip rupture terminates at a larger depth. For a smaller Tohoku-Oki earthquake whose rupture does not reach the accretionary wedge, the sedimentary layer has a slight enhancement effect on the coseismic slip while the accretionary wedge has almost no influence. But the co-existence of the two structures can greatly amplify ground accelerations on the overriding plate. Our 2-D models provide a fundamental understanding of how the low-velocity near-fault structures can impact subduction zone earthquake processes and highlight the importance of considering the effects of accretionary wedges and sedimentary layers in seismic observations and numerical modeling of subduction zone earthquakes.

Data Availability Statement

We used Trelis (https://coreform.com/products/trelisnew/) to mesh the geometrical model. The numerical simulations were solved using SEM2DPACK version 2.3.8 (http://www.sourceforge.net/projects/sem2d/), and simulation results were visualized by Matlab. The input files to reproduce simulation results and the scripts to plot figures in this paper are available on UM Deep Blue (https://doi.org/10.7302/rerb-bd58).

Acknowledgments

X. Li acknowledges the support from China Scholarship Council (NO.201904910712). Y. Huang acknowledges the funding support from the National Science Foundation (Grant Award EAR-1663769). We thank Prithvi Thakur for the helpful suggestions to improve this paper. X. Li also thanks Marlon D. Ramos for helping with the procedures of SEM2DPACK and Trelis.

References

Ampuero, J. P. (2009). SEM2DPACK: A spectral element method tool for 2D wave propagation and earthquake source dynamics, User's Guide, version 2.3.6. Retrieved from http://www.sourceforge.net/projects/sem2d/

Andrews, D. J. (1985). Dynamic plane-strain shear rupture with a slip-weakening friction law calculated by a boundary integral method. *Bulletin of the Seismological Society of America*, 75(1), 1-21.

Brocher, T. M., Fuis, G. S., Fisher, M. A., Plafker, G., Moses, M. J., Taber, J. J., & Christensen, N. I. (1994). Mapping the megathrust beneath the northern Gulf of Alaska using wide-angle seismic data. *Journal of Geophysical Research*, 99(B6), 11663-11685. https://doi.org/10.1029/94JB00111

Brown, L., Wang, K., & Sun, T. (2015). Static stress drop in the Mw 9 Tohoku-oki earthquake: Heterogeneous distribution and low average value. *Geophysical Research Letters*, 42, 10595-10600. https://doi.org/10.1002/2015GL066361

Chu, R., Wei, S., Helmberger, D. V., Zhan, Z., Zhu, L., &Kanamori, H. (2011). Initiation of the great Mw 9.0 Tohoku-Oki earthquake. *Earth and Planetary Science Letters*, 308, 277-283. https://doi.org/10.1016/j.epsl.2011.06.031

Contreras-Reyes, E., Flueh, E. R., & Grevemeyer, I. (2010). Tectonic control on sediment accretion and subduction off south central Chile: Implications for coseismic rupture processes of the 1960 and 2010 megathrust earthquakes. *Tectonics*, 29, TC6018. https://doi.org/10.1029/2010TC002734

Cubas, N., Lapusta, N., Avouac, J.-P., & Perfettini, H. (2015). Numerical modeling of long-term earthquake sequences on the NE Japan megathrust: Comparison with observations and implications for fault friction. *Earth and Planetary Science Letters*, 419, 187-198. https://doi.org/10.1016/j.epsl.2015.03.002

Divins, D. (2003). *Total Sediment Thickness of the World's Oceans & Marginal Seas*. Boulder, CO: NOAA National Geophysical Data Center.

Duan, B. (2012). Dynamic rupture of the 2011 Mw 9.0 Tohoku-Oki earthquake: Roles of a possible subducting seamount. *Journal of Geophysical Research*, 117, B05311. https://doi.org/10.1029/2011JB009124

Flueh, E. R., Fisher, M. A., Bialas, J., Childs, J. R., Klaeschen, D., Kukowski, N., et al. (1998). New seismic images of the Cascadia subduction zone from cruise SO108-ORWELL. *Tectonophysics*, 293, 69-84. https://doi.org/10.1016/S0040-1951(98)00091-2

Fujiwara, T., Kodaira, S., No, T., Kaiho, Y., Takahashi, N., & Kaneda, Y. (2011). The 2011 Tohoku-Oki earthquake: Displacement reaching the trench axis. *Science*, 334, 1240. https://doi.org/10.1126/science.1211554

Fulton, P., Brodsky, E., Kano, Y., Mori, J., Chester, F., Ishikawa, T., et al. (2013). Low coseismic friction on the Tohoku-Oki fault determined from temperature measurements. *Science*, 342, 1214-1217. https://doi.org/10.1126/science.1243641

Gulick, S. P. S., Meltzer, A. M., & Clarke, S. H. (1998). Seismic structure of the southern Cascadia subduction zone and accretionary prism north of the Mendocino triple junction. *Journal of Geophysical Research*, 103(B11), 27207-27222. https://doi.org/10.1029/98JB02526

Gulick, S. P. S., Austin, J. A., McNeill, L. C., Bangs, N. L. B., Martin, K. M., Henstock, T. J., et al. (2011). Updip rupture of the 2004 Sumatra earthquake extended by thick indurated sediments. *Nature Geoscience*, 4, 453-456. https://doi.org/10.1038/ngeo1176

Guo, Y., Koketsu, K., & Miyake, H. (2016). Propagation mechanism of long-period ground motions for offshore earthquakes along the Nankai trough: Effects of the accretionary wedge. *Bulletin of the Seismological Society of America*, 106(3), 1176-1197. https://doi.org/10.1785/0120150315

Holbrook, W. S., Lizarralde, D., McGeary, S., Bangs, N., & Diebold, J. (1999). Structure and composition of the Aleutian island arc and implications for continental crustal growth. *Geology*, 27(1), 31-34. https://doi.org/10.1130/0091-7613(1999)027<0031:SACOTA>2.3.CO;2

Huang, Y., Meng, L., & Ampuero, J.-P. (2012). A dynamic model of the frequency-dependent rupture process of the 2011 Tohoku-Oki earthquake. *Earth, Planets and Space*, 64, 1061-1066. https://doi.org/10.5047/eps.2012.05.011

Huang, Y., Ampuero, J.-P., & Kanamori, H. (2014). Slip-weakening models of the 2011 Tohoku-Oki earthquake and constraints on stress drop and fracture energy. *Pure and Applied Geophysics*, 171, 2555-2568. https://doi.org/10.1007/s00024-013-0718-2

Huang, Y. (2018). Earthquake rupture in fault zones with along-strike material heterogeneity. *Journal of Geophysical Research: Solid Earth*, 123, 9884-9898. https://doi.org/10.1029/2018JB016354

Iinuma, T., Hino, R., Kido, M., Inazu, D., Osada, Y., Ito, Y., et al. (2012). Coseismic slip distribution of the 2011 off the Pacific Coast of Tohoku Earthquake (M9.0) refined by means of seafloor geodetic data. *Journal of Geophysical Research*, 117, B07409. https://doi.org/10.1029/2012JB009186

Ito, Y., Tsuji, T., Osada, Y., Kido, M., Inazu, D., Hayashi, Y., et al. (2011). Frontal wedge deformation near the source region of the 2011 Tohoku-Oki earthquake. *Geophysical Research Letters*, 38, L00G05. https://doi.org/10.1029/2011GL048355

Kaneko, Y., Ito, Y., Chow, B., Wallace, L. M., Tape, C., Grapenthin, R., et al. (2019). Ultralong duration of seismic ground motion arising from a thick, low-velocity sedimentary wedge. *Journal of Geophysical Research: Solid Earth*, 124, 10347-10359. https://doi.org/10.1029/2019JB017795

Kato, N., & Yoshida, S. (2011). A shallow strong patch model for the 2011 great Tohoku-oki earthquake: A numerical simulation. *Geophysical Research Letters*, 38, L00G04. https://doi.org/10.1029/2011GL048565

Kido, M., Osada, Y., Fujimoto, H., Hino, R., & Ito, Y. (2011). Trench-normal variation in observed seafloor displacements associated with the 2011 Tohoku-Oki earthquake. *Geophysical Research Letters*, 38, L24303. https://doi.org/10.1029/2011GL050057

Kimura, G., Hina, S., Hamada, Y., Kameda, J., Tsuji, T., Kinoshita, M., & Yamaguchi, A. (2012). Runaway slip to the trench due to rupture of highly pressurized megathrust beneath the middle trench slope: The tsunamigenesis of the 2011 Tohoku earthquake off the east coast of northern Japan. *Earth and Planetary Science Letters*, 339-340, 32-45. https://doi.org/10.1016/j.epsl.2012.04.002

Klaeschen, D., Belykh, I., Gnibidenko, H., Patrikeyev, S., & von Huene, R. (1994). Structure of the Kuril Trench from seismic reflection records. *Journal of Geophysical Research*, 99(B12), 24173-24188. https://doi.org/10.1029/94JB01186

Kodaira, S., Iwasaki, T., Urabe, T., Kanazawa, T., Egloff, F., Makris, J., & Shimamura, H. (1996). Crustal structure across the middle Ryukyu trench obtained from ocean bottom seismographic data. *Tectonophysics*, 263, 39-60. https://doi.org/10.1016/S0040-1951(96)00025-X

Koketsu, K., Yokota, Y., Nishimura, N., Yagi, Y., Miyazaki, S., Satake, K., et al. (2011). A unified source model for the 2011 Tohoku earthquake. *Earth and Planetary Science Letters*, 310, 480-487. https://doi.org/10.1016/j.epsl.2011.09.009

Kopp, C., Fruehn, J., Flueh, E. R., Reichert, C., Kukowski, N., Bialas, J., & Klaeschen, D. (2000). Structure of the makran subduction zone from wide-angle and reflection seismic data. *Tectonophysics*, 329, 171-191. https://doi.org/10.1016/S0040-1951(00)00195-5

Kopp, H., Flueh, E. R., Klaeschen, D., Bialas, J., & Reichert, C. (2001). Crustal structure of the Central Sunda margin at the onset of oblique subduction. *Geophysical Journal International*, 147, 449-474. https://doi.org/10.1046/j.0956-540X.2001.01547.x

Kozdon, J. E., & Dunham, E. M. (2013). Rupture to the Trench: Dynamic rupture simulations of the 11 March 2011 Tohoku earthquake. *Bulletin of the Seismological Society of America,* 103(2B), 1275-1289. https://doi.org/10.1785/0120120136

Krabbenhöft, A., Bialas, J., Kopp, H., Kukowski, N., & Hübscher, C. (2004). Crustal structure of the Peruvian continental margin from wide-angle seismic studies. *Geophysical Journal International,* 159, 749-764. https://doi.org/10.1111/j.1365-246X.2004.02425.x

Kubo, H., Nakamura, T., Suzuki, W., Dhakal, Y. P., Kimura, T., Kunugi, T., et al. (2019). Ground-motion characteristics and nonlinear soil response observed by donet1 seafloor observation network during the 2016 southeast off-Mie, Japan, Earthquake. *Bulletin of the Seismological Society of America,* 109(3), 976-986. https://doi.org/10.1785/0120170296

Lay, T. (2018). A review of the rupture characteristics of the 2011 Tohoku-oki Mw 9.1 earthquake. *Tectonophysics,* 733, 4-36. https://doi.org/10.1016/j.tecto.2017.09.022

Lotto, G. C., Dunham, E. M., Jeppson, T. N., & Tobin, H. J. (2017). The effect of compliant prisms on subduction zone earthquakes and tsunamis. *Earth and Planetary Science Letters,* 458, 213-222. https://doi.org/10.1016/j.epsl.2016.10.050

Ma, S., & Hirakawa, E. T. (2013). Dynamic wedge failure reveals anomalous energy radiation of shallow subduction earthquakes. *Earth and Planetary Science Letters*, 375, 113-122. https://doi.org/10.1016/j.epsl.2013.05.016

Ma, S., & Nie, S. (2019). Dynamic Wedge Failure and Along-Arc Variations of Tsunamigenesis in the Japan Trench Margin. *Geophysical Research Letters*, 46, 8782-8790. https://doi.org/10.1029/2019GL083148

Mitsui, Y., Kato, N., Fukahata, Y., & Hirahara, K. (2012). Megaquake cycle at the Tohoku subduction zone with thermal fluid pressurization near the surface. *Earth and Planetary Science Letters,* 325-326, 21-26. https://doi.org/10.1016/j.epsl.2012.01.026

Nakanishi, A., Shiobara, H., Hino, R., Kodaira, S., Kanazawa, T., & Shimamura, H. (1998). Detailed subduction structure across the eastern Nankai Trough obtained from ocean bottom seismographic profiles. *Journal of Geophysical Research*, 103(B11), 27151-27168. https://doi.org/10.1029/98JB02344

Noda, H., & Lapusta, N. (2013). Stable creeping fault segments can become destructive as a result of dynamic weakening. *Nature*, 493, 518-521. https://doi.org/10.1038/nature11703

Parsons, T., Trehu, A. M., Luetgert, J. H., Miller, K., Kilbride, F., Wells, R. E., et al. (1998). A new view into the Cascadia subduction zone and volcanic arc: Implications for earthquake hazards along the Washington margin. *Geology*, 26(3), 199-202. https://doi.org/10.1130/0091-7613(1998)026<0199:ANVITC>2.3.CO;2

Sallarès, V., Dañobeitia, J. J., & Flueh, E. R. (2001). Lithospheric structure of the Costa Rican Isthmus: Effects of subduction zone magmatism on an oceanic plateau. *Journal of Geophysical Research*, 106(B1), 621-643. https://doi.org/10.1029/2000JB900245

Sato, M., Ishikawa, T., Ujihara, N., Yoshida, S., Fujita, M., Mochizuki, M., & Asada, A. (2011). Displacement above the hypocenter of the 2011 Tohoku-Oki earthquake. *Science*, 332, 1395. https://doi.org/10.1126/science.1207401

Tsuru, T., Park, J.-O., Miura, S., Kodaira, S., Kido, Y., & Hayashi, T. (2002). Along-arc structural variation of the plate boundary at the Japan Trench margin: Implication of interplate coupling. *Journal of Geophysical Research*, 107(B12), 2357. https://doi.org/10.1029/2001jb001664

Ujiie, K., Tanaka, H., Saito, T., Tsutsumi, A., Mori, J., & Toczko, S. (2013). Low coseismic shear stress on the Tohoku-Oki megathrust determined from laboratory experiments. *Science*, 342, 1211-1214. DOI: 10.1126/science.1243485

von Huene, R., Klaeschen, D., Gutscher, M., & Fruehn, J. (1998). Mass and fluid flux during accretion at the Alaskan margin. *The Geological Society of America Bulletin*, 110(4), 468-482. https://doi.org/10.1130/0016-7606(1998)110<0468:MAFFDA>2.3.CO;2

Wang, K., & Hu, Y. (2006). Accretionary prisms in subduction earthquake cycles: The theory of dynamic Coulomb wedge. *Journal of Geophysical Research*, 111, B06410. https://doi.org/10.1029/2005JB004094

Wells, R. E., Blakely, R. J., Sugiyama, Y., Scholl, D. W., & Dinterman, P. A. (2003). Basin-centered asperities in great subduction zone earthquakes: A link between slip, subsidence, and subduction erosion? *Journal of Geophysical Research*, 108, 2507. https://doi.org/10.1029/2002JB002072

Xie, Z., & Cai, Y. (2018). Inverse method for static stress drop and application to the 2011 Mw9.0 Tohoku-Oki earthquake. *Journal of Geophysical Research: Solid Earth*, 123, 2871-2884. https://doi.org/10.1002/2017JB014871

Yue, H., Lay, T., Rivera, L., An, C., Vigny, C., Tong, X., & Báez Soto, J. C. (2014). Localized fault slip to the trench in the 2010 Maule, Chile Mw = 8.8 earthquake from joint inversion of high-rate GPS, teleseismic body waves, InSAR, campaign GPS, and tsunami observations. *Journal of Geophysical Research: Solid Earth*, 119, 7786-7804. https://doi.org/10.1002/2014JB011340